Experimental Field Investigation of the Effects of Lateral Load Distribution on Concrete Crosstie Track

AREMA 2014 Annual Conference
September 28 – October 1, 2014

Brent A. Williams[1], J. Riley Edwards[2], Marcus S. Dersch[2],
Christopher P. L. Barkan[2], Ryan G. Kernes[3]

Rail Transportation and Engineering Center – RailTEC [2]
Department of Civil and Environmental Engineering
University of Illinois at Urbana-Champaign
205 N. Mathews Ave., Urbana, IL 61801

GIC USA [3]
3333 Lee Parkway, Suite 661
Dallas, TX 75219

4,863 Words, 10 Figures = 7,363 Total Word Count

Brent A. Williams (603) 562-5515 bwillms3@illinois.edu	J. Riley Edwards (217) 244-7417 jedward2@illinois.edu	Marcus S. Dersch (217) 333-6232 mdersch2@illinois.edu
Christopher P.L. Barkan (217) 244-6338 cbarkan@illinois.edu	Ryan G. Kernes (217) 333-6232 rkernes@gic-usa.edu	

ABSTRACT

Increasing freight train axle loads and continued development of high speed rail has placed significant demands on North American rail infrastructure. To adequately address these demands, concrete crosstie and elastic fastening system design and performance must be improved. Field experimentation was conducted at the Transportation Technology Center (TTC) by researchers from the University of Illinois at Urbana-Champaign (UIUC) with the intent of proposing recommendations for improved concrete crosstie fastening system design and performance. The focus of this paper is on quantifying the distribution of lateral forces by use of the Lateral Load Evaluation Device (LLED) developed at UIUC to quantify the loading demands placed on fastening system components (e.g. insulators, clips, shoulders). Loading environment parameters (e.g. magnitudes, location, and train speed) were varied while recording lateral force and displacement measurements at critical interfaces. Other recorded measurements (e.g. vertical loads) are compared and discussed with the intent of investigating potential areas of track instability. Data will be used to improve the understanding of the lateral load path and the effects it has on demands placed on the fastening system. Ultimately, analysis of these data will influence future research on understanding the lateral load path and lead to improved mechanistic design practices for concrete crossties fastening systems.

[1] Corresponding author

INTRODUCTION

The railroad track superstructure is a system designed to safely guide train movement and effectively transfer loads from the wheel to the substructure. A typical track superstructure is comprised of rails, fastening systems, and crossties. The primary functions of the rails are to provide a smooth running surface for the wheels of a train and to distribute wheel loads to the fastening systems and crossties. The fastening system functions to electrically isolate the rail when track circuits are present, distribute wheel loads from the rail into the crosstie, and restrain rail rotation and vertical, lateral, and longitudinal translation. The primary function of the crosstie is to distribute the wheel loads into the substructure and maintain the distance between the two rails, known as track gauge. In North America, pre-cast, pre-stressed concrete crossties are often used the most demanding loading environments including high tonnage, steep grades, and sharp curvature.

Typical North American heavy-haul concrete crosstie fastening systems are comprised of spring clips or clamps, cast-in steel shoulders or screws with dowel inserts, plastic insulators separating the rail from clips and shoulders, and a rail pad assembly between the rail and concrete rail seat. Spring clips and clamps provide the clamping force that holds the rails to the crosstie. Cast-in steel shoulders and screws with dowel inserts provide a hold-down location for the clips and clamps as well as set track gauge. Rail pad assemblies are typically comprised of two parts: a rail pad and an abrasion frame. Their function is to protect the concrete rail seat, distribute vertical wheel loads to the rail seat, and electrically isolate the rail from the crosstie. Insulators serve many functions, including protecting the relatively soft cast-in steel shoulders, transferring lateral wheel loads to the shoulder, transferring clamping forces from the clips to the rails, maintaining track gauge, and electrically isolating the rail from the clips and shoulders.

Electrical isolation is required because typical North American signaling infrastructure uses the rails as track circuits to transmit signals and indicate track occupancy status. The rail must be electrically isolated from the crossties, which are comprised of concrete and steel pre-stressing wires, and steel fastening system components (i.e. conductive materials). The isolation from the rail pad assembly and insulator prevents shunting of the track circuit due to current passing through the crosstie. The plastic rail pad assemblies and insulators become the fastening system's sacrificial wear components due to their lower wear resistance relative to other superstructure materials (i.e. steel and concrete). Wear at key fastening system interfaces has caused premature component failures in demanding loading environments. Failures at the rail seat interface have been studied previously to understand the modes and causes of rail seat deterioration (RSD) and rail pad assembly failure (*1*, *2*). RSD is typically found with worn fastening system components, and is rarely seen on new crossties and fastening systems. This is likely due to the fact that fastening system geometry changes when the rail seat deteriorates. The changes in geometry contribute to excessive stresses and movement in the fastening system, leading to higher demands placed on the rail pad assembly and insulator. RSD, rail pad assembly degradation, and insulator wear are hypothesized to be caused in part by demanding lateral loading conditions. The lateral load path, however, is not well defined. Quantifying the lateral load path in a Safelok I fastening system (Figure 1), which is installed on approximately 16 million of the 27 million North American concrete crossties currently in track on North American Class I railroads, will result in a better understanding of why and how fastening system components fail.

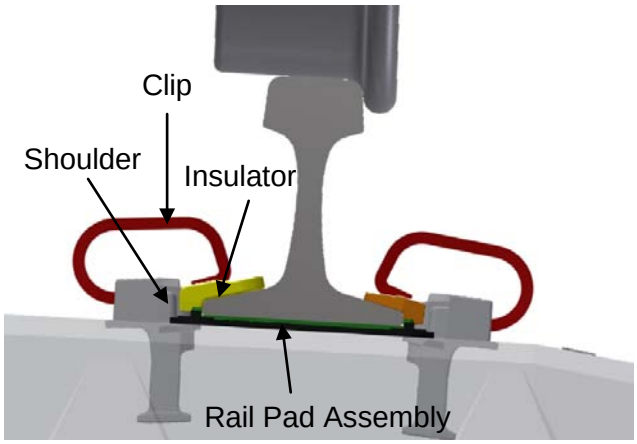

FIGURE 1. Safelok I Fastening System Component Description

The insulator in the fastening system is known to fail when subjected to demanding loading environments (Figure 1). Insulator failure occurs when damage leads to a loss of function of other designed performance characteristics, which includes providing gauge restraint, attenuating the forces entering the shoulder, providing electrical isolation, and transmitting clamping force from the clip to the rail.

The insulator post, the part of the insulator between the rail base and shoulder face (Figure 2), maintains track gauge and is the part of the insulator that fails most frequently. When the insulator post thickness is reduced, failure occurs because the track gauge can widen beyond allowable tolerances. Wide gauge leads to excessive rail movement, further expediting failure mechanisms of other fastening system components or the concrete crosstie. Additionally, insulator post wear has a direct influence on the rate of rail seat abrasion and premature rail pad failure and can lead to wear of the cast-in shoulder (*3*). Insulator failures were first seen by North American railroads in the spring of 1988, just nine months after installation (*4*). Since that time, the life of rail has increased at a rate that exceeds that of the fastening system components. This disparity in life cycles has led to maintenance activities that are focused solely on the fastening system.

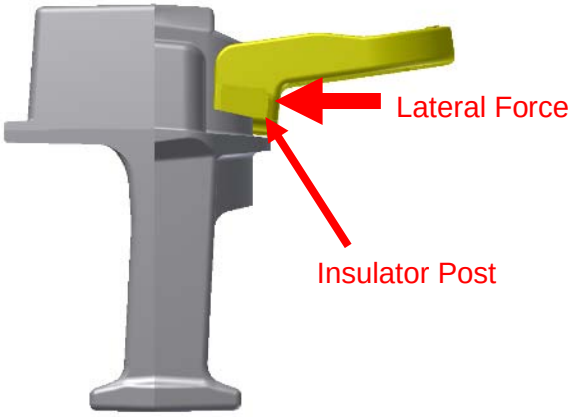

FIGURE 2. Lateral Force Passing Through Insulator Post

A modified Failure Mode and Effect Analysis (FMEA) was used to guide the approach to addressing causes and effects of failed insulators. The FMEA was used to define and identify modes of failure, causes of failure, and effects on other fastening system components and the track system as a whole (*5*). The outcome of the FMEA narrowed the focus of this research to the three primary causes of insulator failure: abrasion, fracturing, and crushing. Abrasion occurs when relative motion occurs between the insulator and the cast iron shoulder or rail base and a force normal to the interface between the surfaces is applied. This relative motion, combined with fines such as sand particles, can degrade the insulator through loss of material on the insulator surface. Fracturing of the insulator can occur when forces are applied that result in cracks due to stress concentrations or brittleness. Lastly, crushing can occur when the lateral force in the insulator post exceeds the strength of the material. Other failure modes such as those caused by environmental conditions can lead to insulator failure. Ultraviolet (UV) light and moisture can alter material properties and initiate failure (*6*). For the reasons listed above, this paper will focus on the causes associated with abrasion, fracturing, and crushing.

Failure modes can have multiple causes. Applied forces and varied geometry characteristics are two primary factors that affect the failure of insulators. Lateral fastening system forces play a role in all three failure modes. Applied forces on the insulator include lateral forces passing through the insulator post and clamping force from the clip. Shear and bending forces applied to the insulator are other forces that can be applied. As a lateral wheel load is applied, lateral displacement of the rail base and insulator post causes the insulator to experience a tensile force due to the clip restraining lateral movement of the insulator. Rail rotation will cause vertical movement of the insulator. Combined with lateral forces passing through the insulator post, frictional forces resisting vertical movement of the insulator will induce shear forces in the insulator leading to abrasion.

Track geometry deviations are often prevalent under demanding loading conditions. As dynamic loads are applied to the track, movement of track components can cause points of load concentration within the fastening system. Skewed crossties can create a concentrated point of load application on the insulator. As the insulator skews, the bearing area that transmits lateral forces from the rail base to the shoulder becomes smaller, increasing the stress in the component. Other component geometry issues include the insulator "walking out" from between the shoulder and rail due to either dynamic loading or movement of the rail. An insulator "walk out" scenario results in complete loss of function of the insulator. Other geometry-induced issues can occur due to poor installation practices. If an insulator is forced into position due to tight tolerances of the fastening system, initial stresses will be imparted into the insulator. When a combination of the limits of fastening system tolerances occurs (e.g. minimum shoulder-to-shoulder distance and maximum insulator post width, or vice versa), high stresses or excessive component movement will result. Insulator failures will likely occur if high applied fastening system forces or severe geometry variations exist. Insulator failures are also likely if high applied fastening system forces and geometry variations occur simultaneously.

The normal force is the lateral force from the rail base passing through the insulator post (Figure 2). Mapping the lateral load path through the fastening system and quantifying the lateral forces passing through the insulator post gives insight into the demands placed on the insulator. Mapping the lateral load path also contributes towards mechanistic design of future components by knowing the location and magnitudes of lateral forces in the fastening system.

Mechanistic design is a process derived from analytical and scientific principles, considering field loading conditions and performance requirements (*7*). To better understand the forces acting on the insulator and how they are distributed, both within the fastening system and globally from crosstie-to-crosstie, researchers at the University of Illinois at Urbana-Champaign (UIUC) have designed the Lateral Load Evaluation Device (LLED). The LLED measures the lateral force passing through the insulator post and entering the shoulder face. The design of individual components within concrete crosstie fastening systems has historically been undertaken through an iterative design process based on practical experience and anecdotal evidence. This type of design process lacks a clear and comprehensive understanding of key design criteria and the mechanical response of components when subjected to load. A more thorough understanding of the mechanical response results from quantifying forces within the fastening system, especially at key interfaces. Quantifying measurements at critical interfaces where failures commonly occur enables researchers to gain a deeper understanding of the demands that components are subjected to under load application. As discussed earlier, there are three main failure modes that have been identified for insulators: crushing, abrasion, and fracturing, all of which require a force normal to the face of the insulator post to initiate failure.

There is large variability among wheel loads in North America due to a variety of factors. Unlike operating conditions in other parts of the world, shared corridor usage between heavy axle load (HAL) freight trains and higher speed passenger trains creates a challenging environment for track component design. These operating environments experience significant load variability, bounded by passenger car wheel loads of 11,000 lbf and HAL freight car wheel loads that can be as high as 39,000 lbf.

In order to best understand the demands imparted on the fastening system, forces at critical interfaces must be quantified under representative loading conditions (i.e. wheel loads). For several decades, wheel impact load detectors (WILDs) have been used to measure vertical wheel-rail interface input loads on tangent track and have been well documented in the literature (*8*). Instrumented sections of rail have also been used to measure lateral wheel-rail interface input loads on curved track and have been well documented in the literature (*9*). Lateral wheel loads are transferred from the wheel, through the rail, and into the fastening system. Lateral forces at critical interfaces in the fastening system, however, have not been quantified to the same extent. This paper presents a method of quantifying lateral forces in the fastening system as they pass from the base of the rail through the insulator and are resisted by the shoulder. With track infrastructure parameters (e.g. components and geometry) held constant, lateral forces at the critical insulator-shoulder interface directly beneath the point of loading are hypothesized to resist a constant percentage of the lateral wheel load. HAL freight trains are hypothesized to impart higher lateral forces in the fastening system than passenger trains. The results of this study will provide a more thorough understanding of the effects of a varied loading environment, aiding in a mechanistic design approach for future fastening systems and their components.

LATERAL FORCE MEASUREMENT TECHNOLOGY

Researchers at UIUC developed a technology to measure the lateral force at the insulator-shoulder interface while maintaining the original geometry of a concrete crosstie Safelok I fastening system. This approach was developed after learning from earlier, less successful experimental attempts to measure the lateral force passing through the insulator post and entering the shoulder. UIUC's LLED has two defined points of contact with the shoulder that act as outer supports and two defined points of contact with the insulator that are narrower than the supports. Together, this specific geometric configuration induces a bending action of the beam under load. The beam contains four strain gauges which are wired into a full Wheatstone Bridge to measure bending strain under load. Two strain gauges are applied horizontally one inch from the center of the beam to measure compressive strains (Figure 3a). The locations of the gauges are between the points of contact with the insulator, to reduce the liklihood of the gauges being damanged. The other two strain gauges are applied horizontally one inch from the center of the beam between the two supports to measure tensile strains (Figure 3b). The face of the cast fastening system shoulder is ground away using a handheld grinder and straight edge to ensure the original dimensions are maintained.

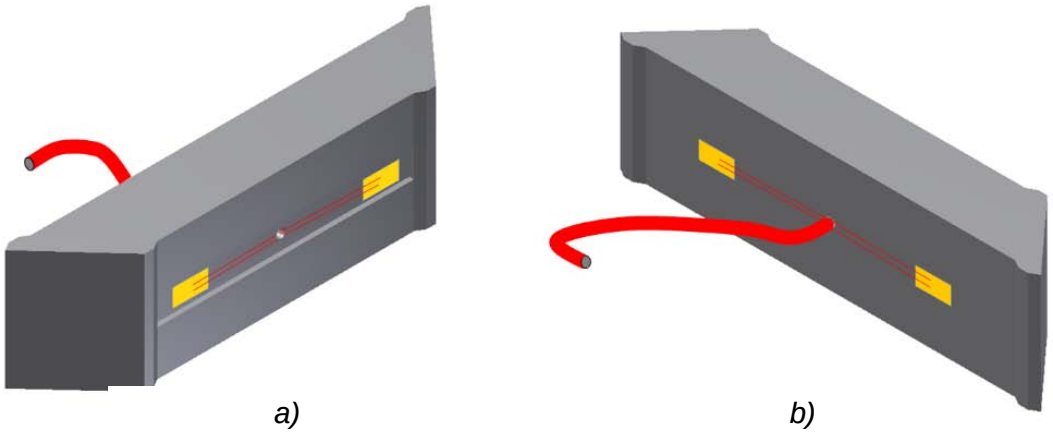

a) *b)*

FIGURE 3. LLED Strain Gauge Location and Orientation

Once the shoulder face is ground away, the LLED replaces it (Figure 4). The primary advantage of this technology is that all of the orignal fastening system geometry is maintained, thus clip installation procedures and all fastening system components remain the same. The LLED material and geometry were also designed to reduce experimental error caused by different stiffnesses than the original configuration. Because lateral restraint is one of the fasteing system's primary functions, the LLED also will allow us to understand how variables associated with friction (e.g. materials and geometry) alter the lateral load path in addition to the magnitudes of lateral fastening system forces (*10*). Therefore, data obtained by the LLED will aid future fastening system design by quantifying the lateral loads.

FIGURE 4. LLED Installed in Fastening System

LLED strains are suqsequently resolved into a force through the use of calibration curves generated prior to testing using a uniaxial loading frame. For calibration, LLEDs were supported on a level plate by two small steel blocks and loaded with a self-leveling loading head to ensure perpendicular loading. Loads were applied in 1,000 pound (1 kilopound (kip)) increments throughout the range of expected magnitudes in the field while corresponding strains were recorded. A thin steel insert is placed between the insulator and the two points of contact on the beam to ensure the points of loading would not penetrate into the relatively soft insulator material (Nylon 6/6). If this did happen, it would turn the two-point load into a distributed load, negatively impacting the accuracy of the results (*6*). The stiffness of the beam and insert were chosen such that the stiffness of the system remained similar to its original conditions. The end result is a load cell at the shoulder-insulator interface that preserves the original geometry and ensures that the load path within the fastening system remains unaffected.

Initial proof-of-concept testing of the LLED was conducted in the labotatory. Laboratory testing was conducted on the Pulsating Load Testing Machine (PLTM) (*11*). Figure 5 shows data from part of a dynamic LLED test test at 3 Hertz (Hz) with a maximum vertical load of 32,500 lbf and a minimum load of -1,000 lbf at a constant L/V ratio of 0.5. Dynamic tests simulated a train pass. As Figure 5 shows, high resolution data were captured, confirming the technology was a viable option to implement in the field.

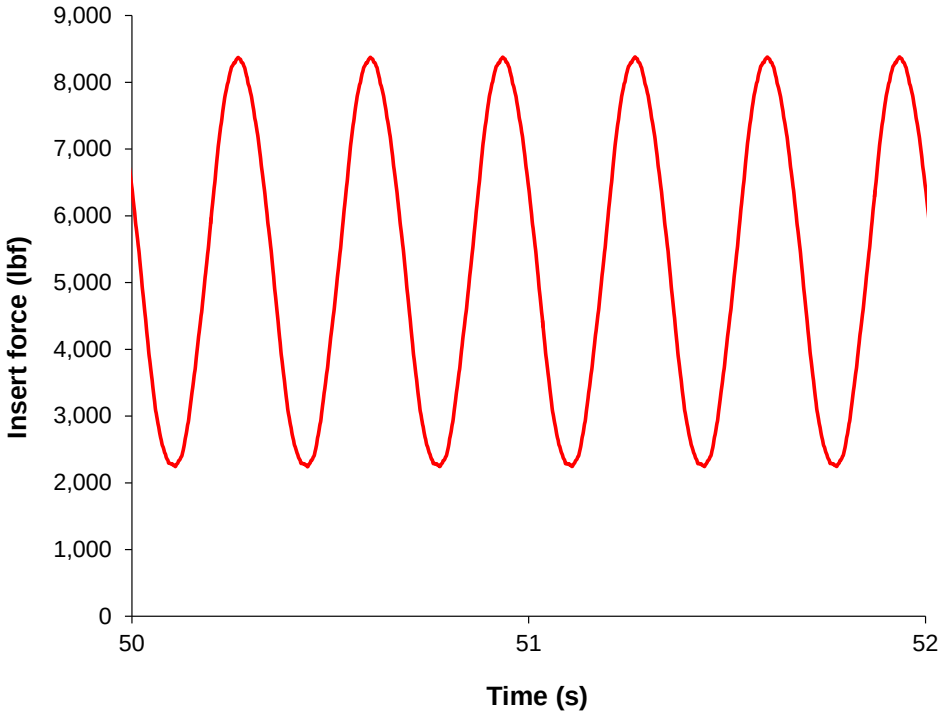

FIGURE 5. Preliminary Dynamic LLED Laboratory Test – Constant L/V = 0.5, Max./Min. Vertical Load = 32,500/-1,000 lbf, Freq. = 3 Hz

FIELD EXPERIMENTATION SETUP

Field experimentation was conducted at the Transportation Technology Center (TTC) in Pueblo, Colorado. Field experiments and results described in this paper were conducted on a segment of tangent track on the Railroad Test Track (RTT) and a segment of curved track on the High Tonnage Loop (HTL) at TTC. Different loading scenarios (e.g. load magnitudes, L/V ratios, etc.) were applied to the track using the Track Loading Vehicle (TLV). The TLV uses a deployable axle capable of applying various combinations of vertical and lateral loads to simulate typical track loading conditions. Two types of trains were also used to measure the lateral response of the fastening system under dynamic and impact loading conditions on the HTL at speeds of 2, 15, 30, 40, and 45 mph. A train consisting of one six-axle locomotive and nine passenger cars was used to simulate the dynamic loading of a passenger train. A train consisting of three six-axle locomotives and ten freight cars of varying weights was used to simulate the dynamic loading of a freight train. Both test track sections consisted of a 136RE rail section, concrete crossties spaced at 24 inches center-to-center, Safelok I type fastening systems, and premium ballast. LLEDs were installed on the field side of the rail on both rail seats of three adjacent concrete crossties. Figure 6 shows the location and naming convention of instrumentation on both test sections. Data was recorded at a sampling rate of 2,000 Hertz to maximize the number of samples taken during each static and dynamic test.

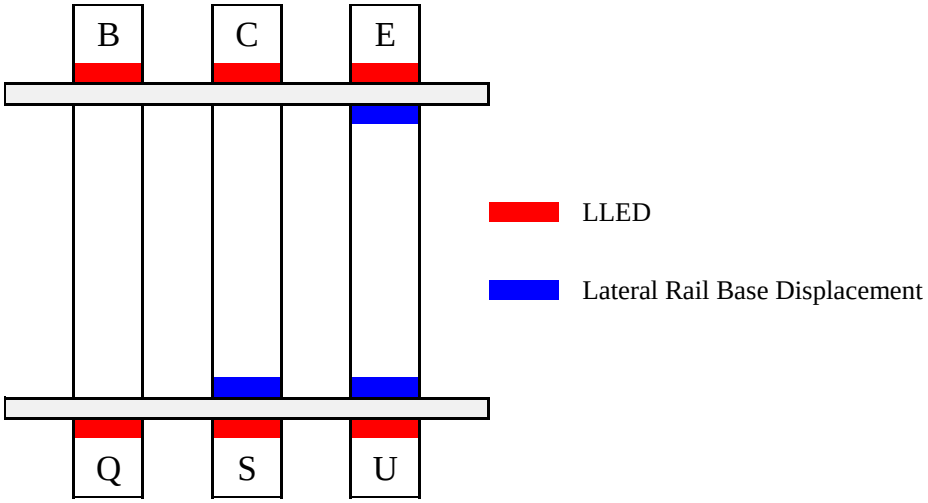

FIGURE 6. Instrumentation Location

INFLUENCE OF LATERAL AND VERTICAL WHEEL LOADS

The RTT was chosen for static testing to minimize variability due to vehicle-track dynamics in the curve. The LLED at rail seat Q on the RTT was compromised during static testing, making any data gathered from the LLED unreliable. However, rail seats B, C, E, S, and U functioned properly (Figure 6). Data from the five functioning rail seats were analyzed to understand the influence of lateral wheel loads on lateral fastening system forces. Figure 7 shows the average magnitude of lateral forces measured by the LLEDs for given lateral wheel loads and a 40 kip vertical wheel load applied by the TLV directly over the specified rail seat.

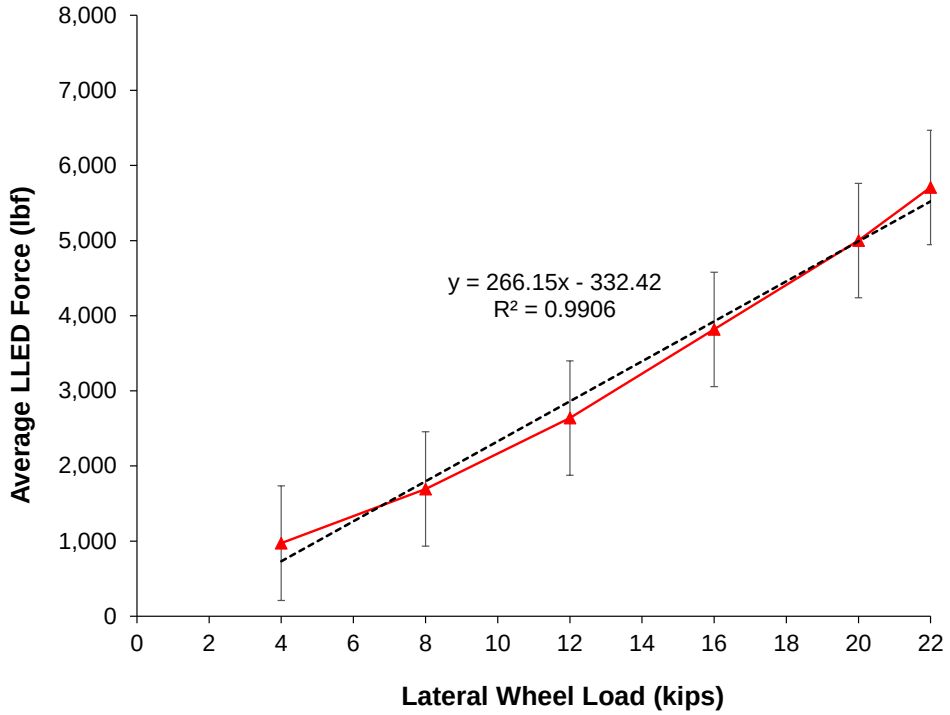

FIGURE 7. Average LLED Force Under Static 40 kip Vertical Wheel Load

The average LLED force from static TLV loading was plotted against various lateral wheel loads under a constant 40 kip vertical wheel load to determine the load transfer characteristics of the system (Figure 7). As lateral wheel loads increased, the average LLED force on the rail seat directly beneath the

point of loading increased linearly. A linear trend line of the average LLED force data shows that approximately 266 lbf will be transferred into the shoulder per one kip of lateral wheel load. The data also indicate that approximately 26% of the lateral wheel load will be transferred into the shoulder regardless of the magnitude of the lateral wheel load.

The average LLED force from static TLV loading was also plotted against various lateral wheel loads under constant 20 kip and 40 kip vertical wheel load to determine the load transfer characteristics of the system under varying vertical wheel loads (Figure 8). As lateral wheel loads increased, the average LLED force under both vertical wheel load magnitudes on the rail seat directly beneath the point of loading increased linearly. A linear trend line of the average LLED force data for all data points shows that approximately 250 lbf will be transferred into the shoulder per one kip of lateral wheel load. The data indicate that approximately 25% of the lateral wheel load will be transferred into the shoulder regardless of the magnitude of the lateral wheel load. The data also indicate that vertical wheel load has little to no effect on the lateral load transfer characteristics of the system.

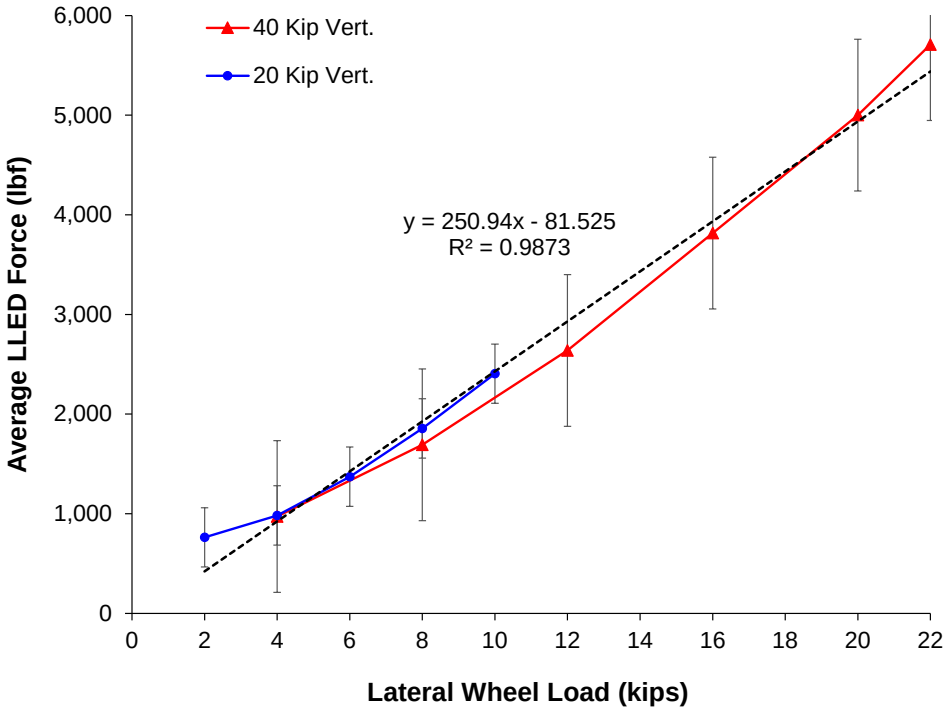

FIGURE 8. Average LLED Force Under Static 20 kip and 40 kip Vertical Wheel Load

All dynamic train test data described in this paper is from rail seat U on the low rail and rail seat E on the high rail of the HTL test section. Rail seats U and E were chosen to maintain a constant location while being able to compare rail seats on the same crosstie under varying dynamic loading scenarios. The peak LLED forces from axles of dynamic freight car loading were also plotted against the corresponding applied lateral wheel loads under speeds ranging from 2 mph to 45 mph to determine the load transfer characteristics of the system under varying speeds and constant car weight (Figure 9). As lateral wheel loads increased, the corresponding peak LLED forces from the axles of the freight train increased relatively linearly. A linear trend line of the peak LLED force data for all data points shows that approximately 330 lbf will be transferred into the shoulder per one kip of lateral wheel load on rail seat U and 420 lbf will be transferred into the shoulder per one kip of lateral wheel load on rail seat E. The data indicate that approximately 33% of the lateral wheel load will be transferred into the shoulder on rail seat U and 42% of the lateral wheel load will be transferred into the shoulder on rail seat E, a difference of 9%. A variety of factors could have led to the difference in percentage of load transferred to the shoulder. Differences in loading conditions (i.e. static vs. dynamic) can have an effect on the magnitudes of the applied wheel loads. Differences in track geometry (i.e. tangent vs. curved) will also have an effect on the vehicle-track interaction causing variances in magnitudes of the applied wheel loads. Although the data cannot be directly compared due to different testing locations (RTT vs. HTL), it can be noted that rail seat U on the

low rail of the HTL behaved similarly to the averaged data from the RTT. However, rail seat E on the high rail of the HTL produced much higher magnitudes of lateral bearing forces than the remaining data. The relatively linear relationship between the force imparted into the shoulder and applied lateral wheel load shows that a constant percentage of the lateral wheel loads can be used to estimate the forces transferred to the shoulder throughout the wide range of applied lateral wheel loads that can occur in field service. A linear trend may underestimate forces on the shoulder at higher lateral wheel loads, and warrants future investigation into a more accurate way of correlating forces on the shoulder and lateral wheel loads.

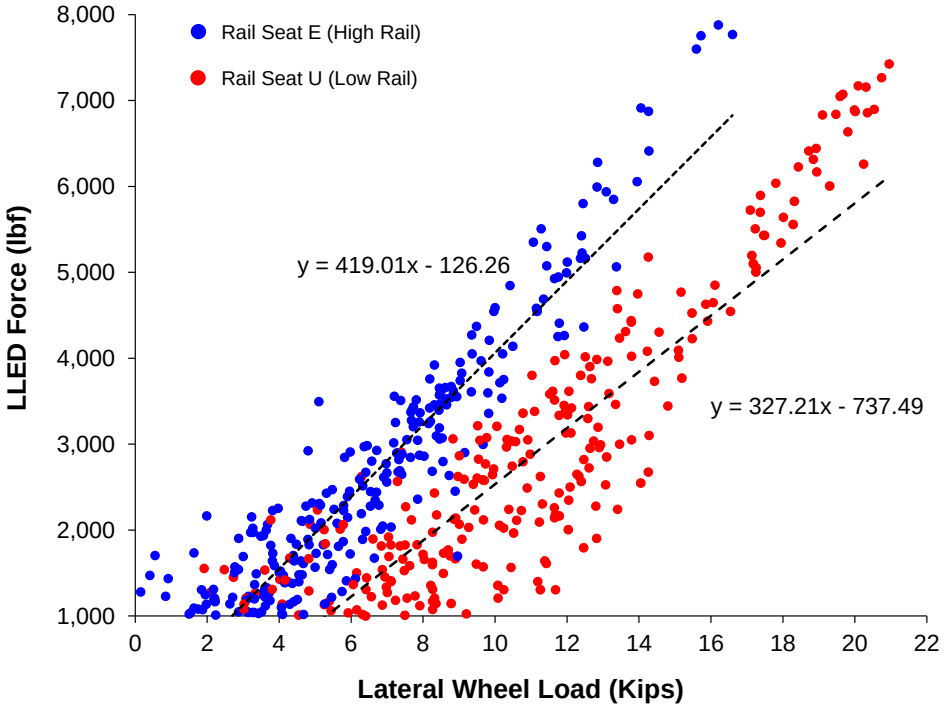

FIGURE 9. Peak LLED Forces Under HAL Freight Train as a Function of Lateral Wheel Load

INFLUENCE OF TRAIN CONSIST TYPE

By definition, shared corridors see a variety of rolling stock types. To better understand the lateral demands on the shoulder that different types of rolling stock impart on the track, passenger and freight consists are compared. Figure 10 shows peak LLED forces from various speeds during dynamic freight and passenger train tests. The maximum LLED forces for passenger cars were consistently significantly lower than the magnitudes measured from freight cars (Figure 10). All lateral forces measured by the LLED were less than 1,000 lbf. At 15 mph, lateral forces measured by the LLED on rail seat U on the low rail were 618 lbf for the passenger consist while the freight consists yielded 6,637 lbf, more than an order of magnitude higher than the passenger consist. At 15 mph, lateral forces measured by the LLED on rail seat U on the low rail were 618 lbf for the passenger consist while the freight consists yielded 6,637 lbf, more than an order of magnitude higher than the passenger consist. Lower magnitudes of loads from passenger trains were consistent at all speeds. The lower magnitudes indicate that passenger trains impart lateral demands on the fastening that are significantly lower than freight trains. Although the forces from the freight consist were about ten times larger than those from the passenger consist, the freight car weights were only approximately 3.7 times heavier than the passenger cars. The disparity indicates that an increase in car weight of approximately 400% could result in an increase in lateral fastening system forces of approximately 1,000%. The disparity also indicates that due to their inherently higher car weights, freight consists impart much higher forces in the fastening system than passenger consists.

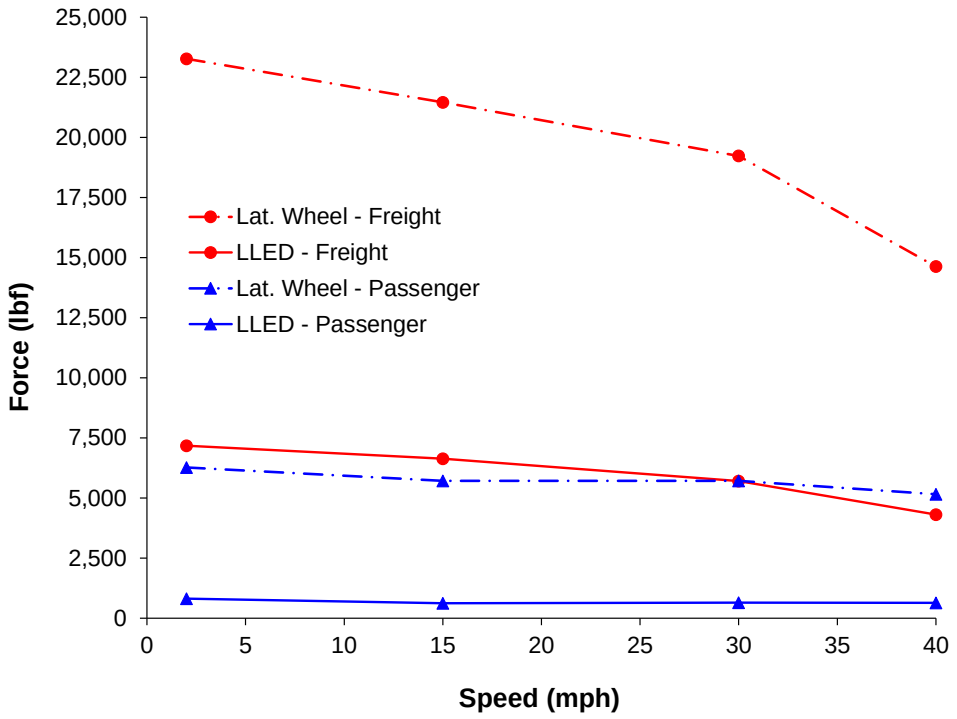

FIGURE 10. Maximum Lateral Wheel Loads and LLED Forces as a Function of Speed

The decreasing trend in the data is due to the location of the instrumentation. Because rail seat U is on the low rail of the curve, the increasing outward force of the train with increasing speed causes the low rail to withstand lower forces. Train dynamics will govern the steering charactersitics of a train through a curve, which warrants addional discussion that is outside the scope of this paper. However, the data can still be investigated. As speed increased, both lateral wheel loads and LLED forces decreased. Figure 9 indicates rail seat U tranferred approximately 35% of the lateral wheel loads to the shoudler. From Figure 10, the same trend can be observed. The percentage of lateral wheel loads transferred to the shoulder at 2, 15, 30, 40, and 45 mph was 34.5%, 33.5%, 32.8%, 31.5%, and 30.8%, respectively. The percentages futher indicate a relatively linear trend between the forces entering the shoulder and the lateral wheel loads.

CONCLUSIONS AND FUTURE WORK

The following conclusions can be drawn from the analysis of data collected in these field experiments using LLEDs:

- Lateral fastening system forces acting on the shoulder face appear to be primarily related to the lateral wheel load, regardless of the vertical wheel load.

- An increase in lateral wheel load of approximately 400% (i.e. four times) can result in an increase in lateral fastening system forces of approximately 1,000% (i.e. ten times),

- Passenger trains exert approximately an order of magnitude (i.e. ten times) less lateral force than heavy axle load (HAL) freight trains. It should be noted that wheels from the freight train were likely conformal to the rail head profile due to accelerated testing, whereas the passenger train likely had a wheel profile much different than the rail profile, possibly resulting in lower passenger train forces. It should also be noted that dynamic tests were run with approximately four inches of cant deficiency and that all freight cars were loaded.

- Approximately 25-40% of the lateral wheel load can be transferred to the shoulder face directly beneath the point of loading. However, a linear trend may underestimate forces on the shoulder at

higher lateral wheel loads, and warrants future investigation into a more accurate way of correlating forces on the shoulder and lateral wheel loads.

Given the steady increase in North American concrete crosstie usage, research at UIUC will continue to develop a comprehensive laboratory and field experimentation plan to better understand the lateral load path and lateral fastening system demands. The static experiments described in this paper were theoretical in nature, with the loading conditions chosen by researchers based on expert opinion and working knowledge rail seat loads.

Future laboratory and field experimental testing will include installing LLED-type instrumentation on rail seats of concrete crossties with different types of fastening systems to better understand the effect that variations in fastening system design have on the lateral load path and lateral fastening system demands. Laboratory and field testing will also be conducted on crossties and fastening systems with various degrees of rail seat deterioration (RSD) and/or epoxy coated rail seats to investigate the effect of frictional characteristics of the fastening system on the lateral load path. Future testing will also include measuring lateral fastening system forces on both the field and gauge sides to understand the effects of hunting of narrow gauge scenarios.

Field testing on revenue-service Class I railroad track will play a critical role in guiding future laboratory experimentation on UIUC's full-scale Track Loading System (TLS). A working relationship between field data and experimental laboratory data is expected as the lateral load path of various fastening system types becomes more refined and more realistic field conditions are simulated in the laboratory.

The use of LLEDs appears to be a novel technique to instrument concrete crosstie fastening systems to characterize the lateral load and accurately quantify the lateral fastening system demands. Results from this work will be leveraged, as the data collected from LLEDs in the laboratory and field experiments will be used as validation of UIUC's finite element (FE) analysis of the concrete crosstie and fastening system.

ACKNOWLEDGEMENTS

This project is sponsored by a grant from the Association of American Railroads (AAR) Technology Outreach Program with additional funding for field experimentation provided by the United States Department of Transportation (DOT) Federal Railroad Administration (FRA). The published material in this paper represents the position of the authors and not necessarily that of DOT. The authors would like to thank Dave Davis of AAR/TTCI and the members of the AAR Technology Outreach Committee; John Bosshart and Thomas Brueske of BNSF; Harold Harrison of H2 Visions, Inc.; Don Rhodes and Bill Rhodes of Instrumentation Services, Inc.; Tim Prunkard, Darold Marrow, and Don Marrow of the University of Illinois at Urbana-Champaign (UIUC); Jose Mediavilla of Amsted RPS; Jim Beyerl of CSX Transportation; Steve Ashmore and Chris Rewczuk of UPRR; and Bob Coats of Pandrol USA for their advice, guidance and contributions to this research. The authors would also like to acknowledge Daniel Kuchma, David Lange, Thiago Bizarria, Christopher Rapp, Brandon Van Dyk, Sihang Wei, Justin Grasse, Kartik Manda, and Andrew Scheppe from UIUC for their work on this research. J. Riley Edwards has been supported in part by the grants to the UIUC Railroad Engineering Program from CN, Hanson Professional Services, and the George Krambles Transportation Scholarship Fund.

REFERENCES

(1) Zeman, John C. 2010. *Hydraulic Mechanisms of Concrete-Tie Rail Seat Deterioration*. Urbana. University of Illinois at Urbana-Champaign.

(2) Bizarria, Thiago, J. Riley Edwards, Ryan Kernes, Christopher P. L. Barkan, and Bassem Andrawes. 2014. "Mechanistic Behavior of Concrete Crosstie Fastening System Rail Pad Assemblies." *Proceedings: Transportation Research Board Annual Conference*. Washington D.C.: Transportation Research Board.

(3) 2012. "AREMA Manual for Railway Engineering." Ch. 30, Parts 1 and 4. Maryland: American Railway Engineering and Maintenance of Way Association.

(4) Bosshart, John, interview by Brent Williams. 2012. *Insulator Deterioration* (October 26).

(5) Stamatis, D. H. 1995. *Failure Mode and Effect Analysis: FMEA From Theory to Execution.* Milwaukee: ASQC Quality Press.

(6) Painter, Paul C. 2011. *Essentials of Polymer Science and Engineering.* Lancaster: DEStech Publications, Inc.

(7) Van Dyk, Brandon, J. Riley Edwards, Conrad J Ruppert, and Christopher P. L. Barkan. 2013. "Considerations for Mechanistic Design of Concrete Sleepers and Elastic Fastening Systems in North America." *Proceedings of the 2013 International Heavy Haul Association Conference* . New Delhi: International Heavy Haul Association.

(8) Van Dyk, Brandon. 2012. *International Concrete Crosstie and Fastening System Survey - Final Results.* Survey Results, Urbana: University of Illinois at Urbana Champaign.

(9) Grasse, Justin. 2013. *Field Test Program of the Concrete Crosstie and Fastening System.* Urbana: University of Illinois at Urbana Champaign.

(10) Czichos, H. 1978. *Tribology: A Systems Approach to the Science and Technology of Friction, Lubrication, and Wear.* New York: Elsevier North-Holland, Inc.

(11) Rapp, Christopher T, Marcus S Dersch, Christopher P. L. Barkan, and Jose Mediavilla. 2013. "Measuring Concrete Crosstie Rail Seat Pressure Distribution with MAtrix Based Tactile Surface Sensors." *Proceedings: Transportation Research Board Annual Meeting.* Wasington D.C.: Transportation Research Board. 2-3.

FIGURES

Experimental Field Investigation of the Transfer of Lateral Wheel Loads on Concrete Crosstie Track

AREMA Annual Conference

Chicago, IL

30 September 2014

Brent A. Williams, J. Riley Edwards, Marcus S. Dersch

Presentation Outline

- FRA project overview
- Motivation for research
- Experimentation overview
- Measurement technology
- Effects of varying vertical loads
- Dynamic effect on lateral loads
- Conclusions and future work

FRA Tie and Fastening System BAA Objectives and Deliverables

- **Program Objectives**
  - Conduct comprehensive state-of-the-art design and performance assessment via international literature review
  - Execute laboratory and field experimentation to better define demands at critical interfaces as well as validate a finite element (FE) model
  - Update current design recommended practices where applicable

U.S. Department of Transportation
Federal Railroad Administration

FRA Tie and Fastener BAA Industry Partners:

UNION PACIFIC
BUILDING AMERICA
BNSF RAILWAY
AMTRAK
Amsted RPS
An Amsted Rail Company
GIC
GIC INGENIERÍA Y CONSTRUCCIÓN S.A. DE C.V.
HANSON
LB Foster
CXT Concrete Ties
TTX

Overall Project Deliverables

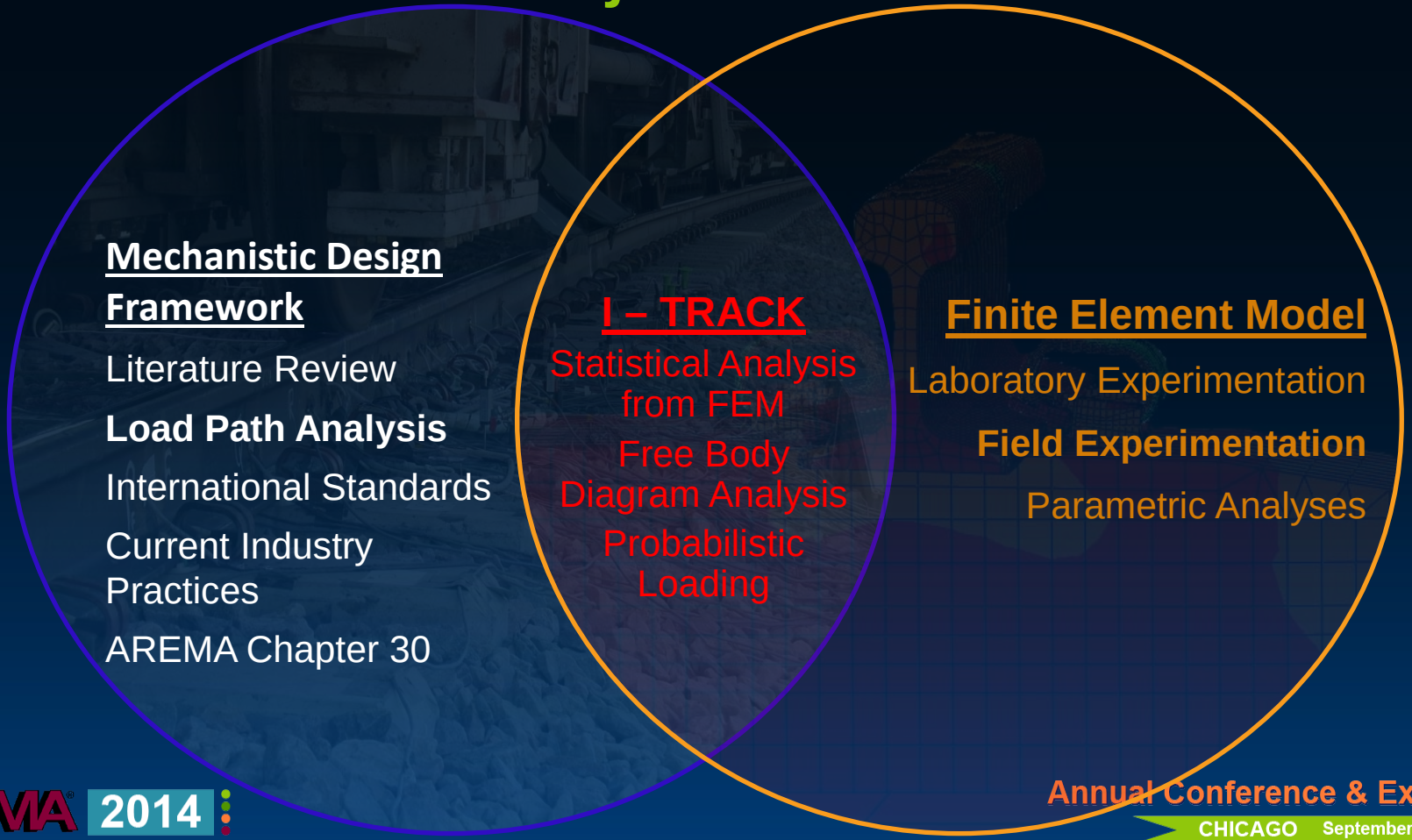

FRA Project – Greatest Impacts

- Improved understanding into the:
  - Current North America shared corridor loading environment through wheel impact load detector (WILD) data mining
  - Lateral load path through the development of a novel lateral load measurement device
  - Critical design parameters through the development of a validated multi-crosstie and fastening system 3D FE model
  - Pressure distribution at the rail seat, as well as other information through the successful field and laboratory experimentation
- Development of a full-scale laboratory track loading system
- For more information, please visit:
  - *ict.uiuc.edu/railroad/CEE/crossties/downloads.php*

Motivation for Research

- The lateral load path was not well defined
- Lateral loads can contribute to premature fastening system component failure
- Data acquired will provide railroads and suppliers information for future fastening system designs
  - i.e. mechanistic design approach of fastening system components
- ~60% of North American concrete crossties in service today use Safelok I type fastening system

Field Experimental Program

- **Objective:** Analyze the distribution of forces through the fastening system and impact on components relative displacements
- **Location:** Transportation Technology Center (TTC) in Pueblo, CO
  - **Railroad Test Track (RTT):** tangent section
  - **Heavy Tonnage Loop (HTL):** curved section
- **Instrumentation:**
  - Lateral load evaluation devices
  - Potentiometers to capture rail base lateral displacement
- **Loading:** Track Loading Vehicle (TLV) used to apply static loads to the track structure
  - Modified railcar with instrumented wheelset on hydraulic actuators

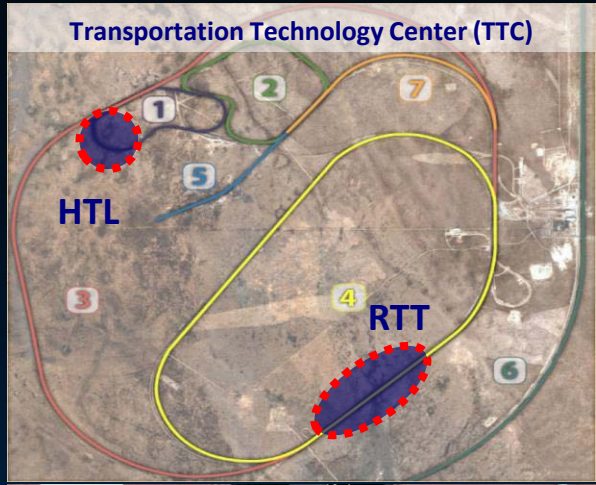

Measurement Technology

Lateral Load Evaluation Device (LLED)

- Replaces original face of cast shoulder
- Maintains original fastening system geometry
- Designed as a beam in four-point bending
- Bending strain is resolved into force through calibration curves generated in the lab

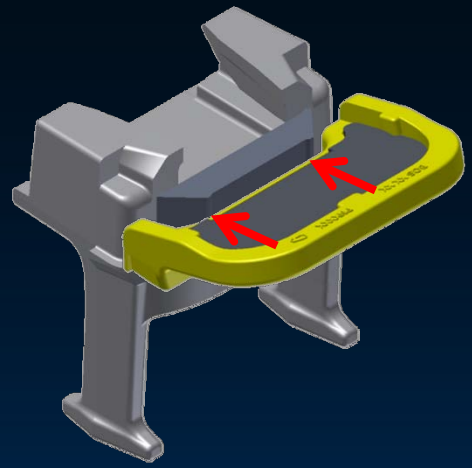

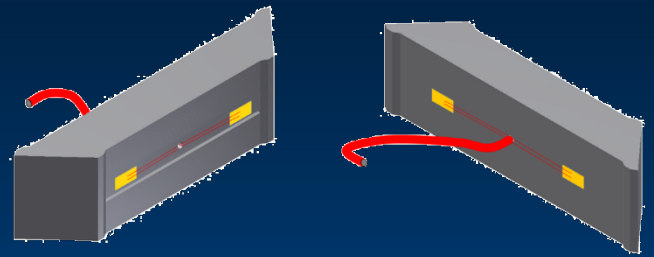

Instrumentation Layout

High Rail (HTL)

Low Rail (HTL)

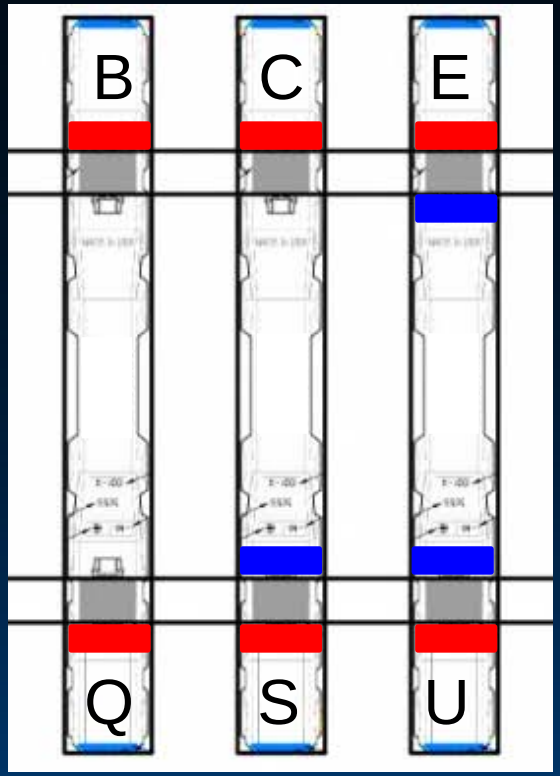

LLED

Lateral Rail Base Potentiometer

Defining the Lateral Load Path

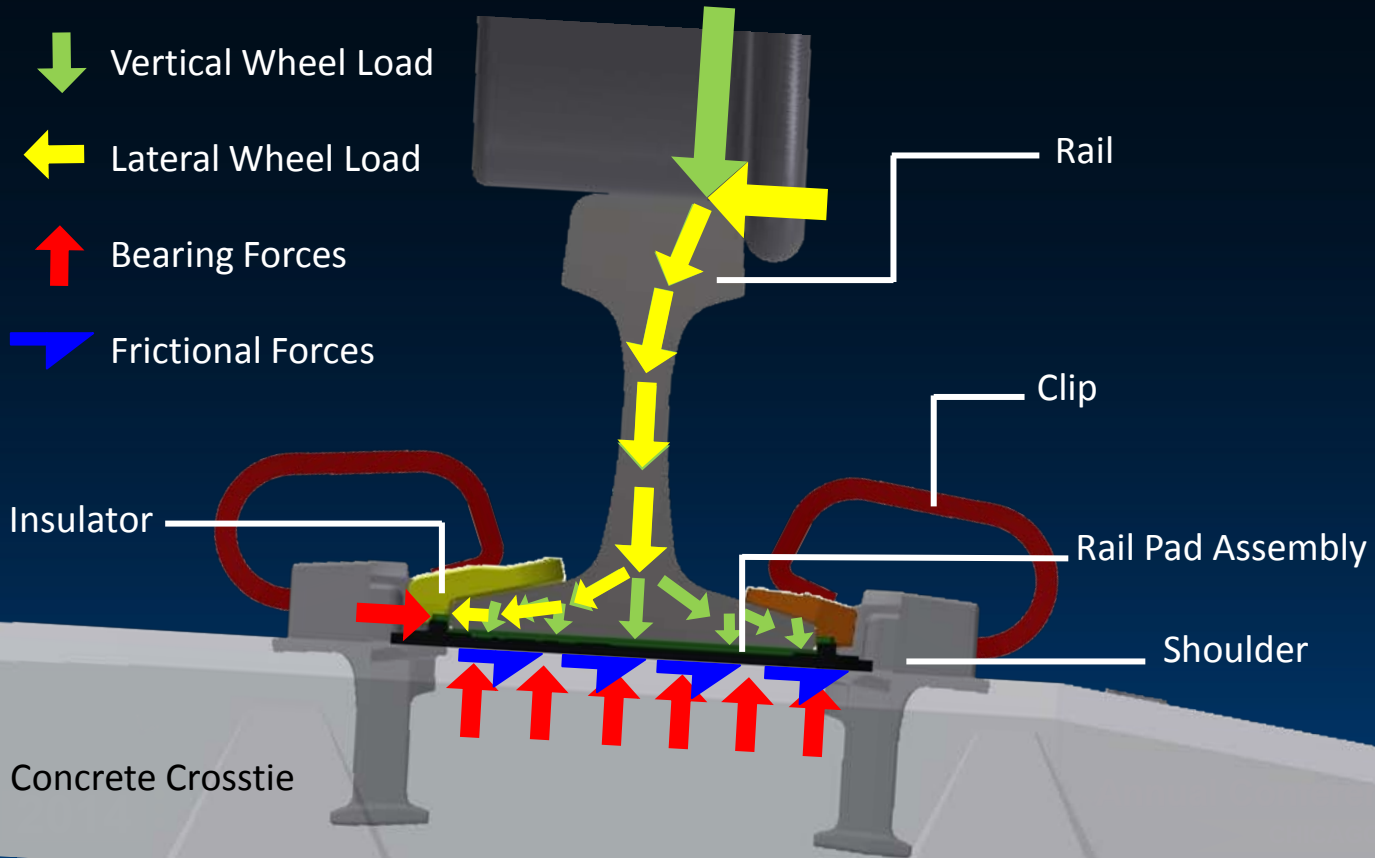

Lateral Load Model Equations for Analysis

$\Sigma L_L = \Sigma L_B + \Sigma L_F$

where,

ΣL_L = Total lateral load

ΣL_B = Lateral bearing force

ΣL_F = Lateral frictional force

$F_F = \mu N$

where,

F_F = Frictional Force

μ = Coefficient of Friction

N = Normal Force

Effect of Varying Vertical Load

Assume load distribution of: 50% bearing, 50% friction

If $L_L = \Sigma L_B + \Sigma L_F$, then $\Sigma L_L = \Sigma L_B + \Sigma(\mu N)_{\text{rail seat}}$

where,

μ = Coefficient of Friction between rail pad and rail seat

N = Force normal to frictional plane (vertical wheel load)

If N decreases by 50%, then load distribution changes to:
75% bearing, 25% friction

Effect of Varying Vertical Load:
Total Lateral Forces in Track*

- 20 kip and 40 kip vertical wheel load tests produce extremely similar results
- Frictional and bearing forces start to converge as lateral wheel load increases
- Trend does not agree with $F_F = \mu N$ equation

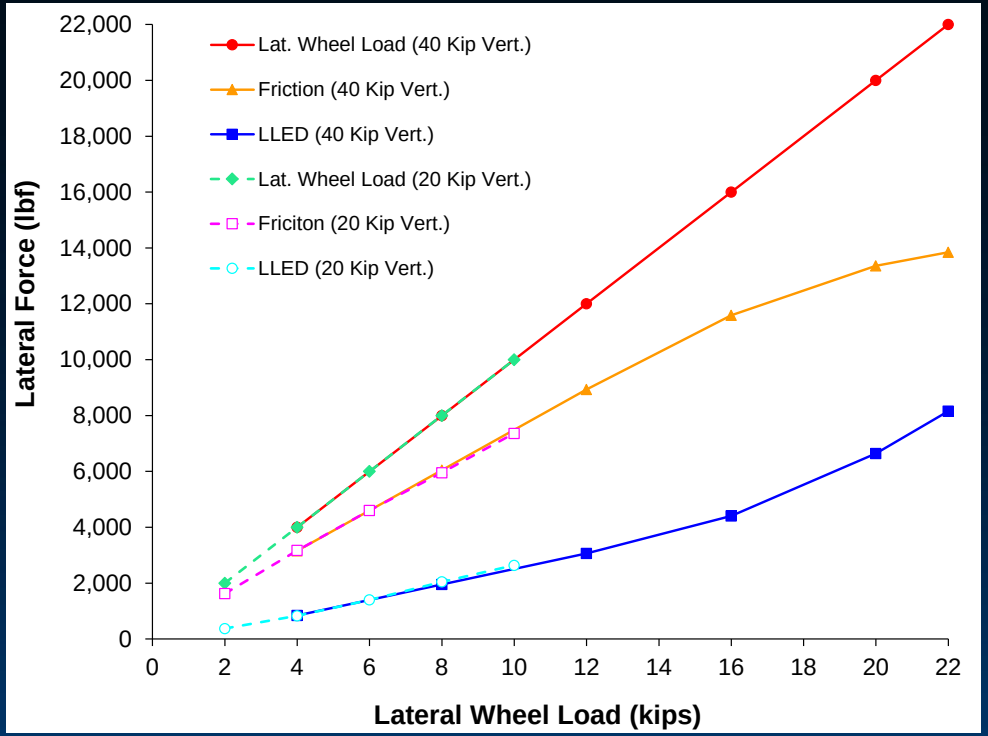

*Sum of three adjacent rail seats (B, C, E)

Effect of Varying Vertical Load

Average for Single Rail Seat*

- Difference between lines:
  - increases as lateral wheel load increases
  - likely due to the lower normal force (vertical wheel load) applied to the rail seat
- Trend does not agree with theoretical equations

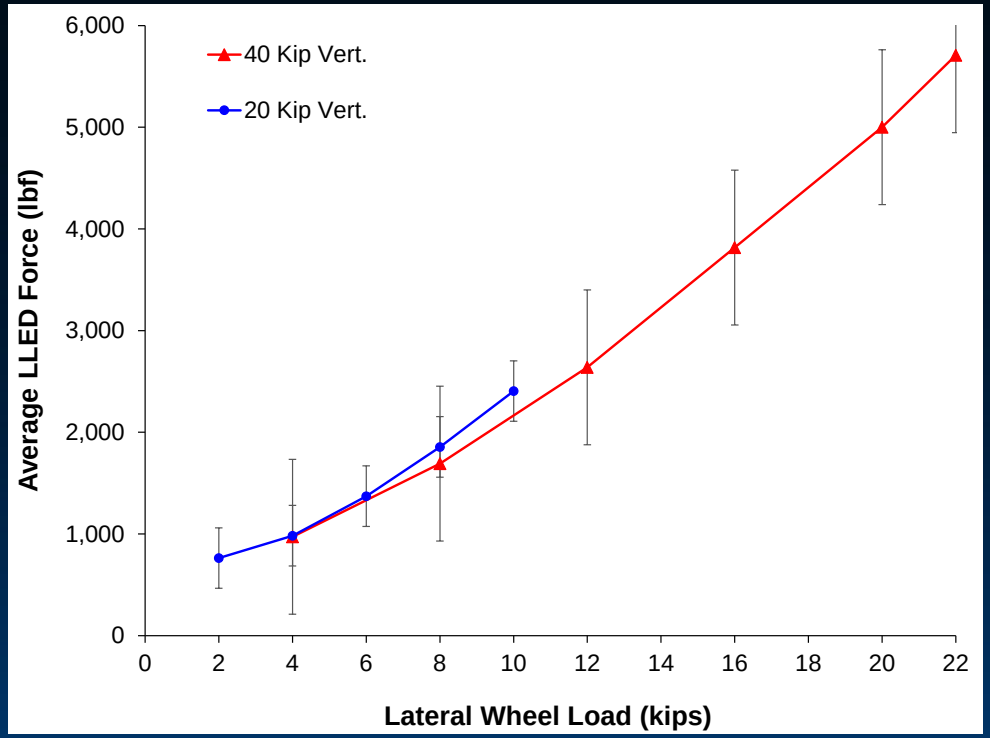

*Average from static tests on five rail seats (B, C, E, S, U)

Effect of Varying Lateral Load

Average for Single Rail Seat*

- As lateral wheel load increases
  - ratio of frictional force to bearing force decreases from 3.7 to 1.7, or 54%
  - percent bearing force increases from 21% to 37%

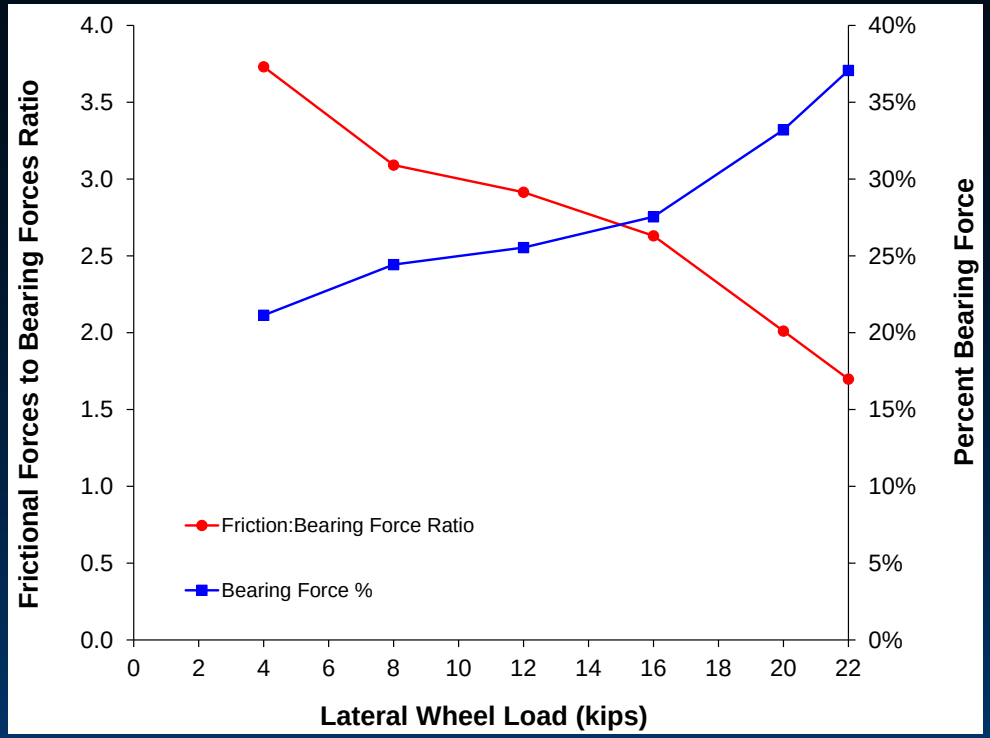

*Average from static tests on five rail seats (B, C, E, S, U)

Longitudinal Distribution of Lateral Loads

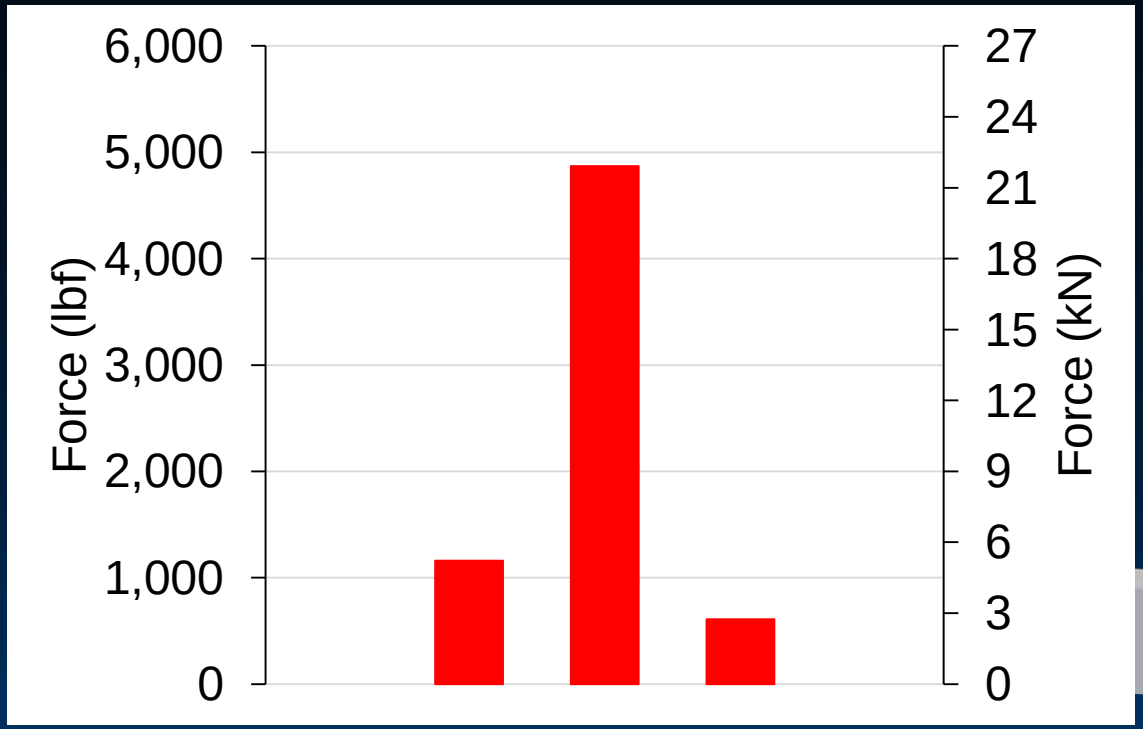

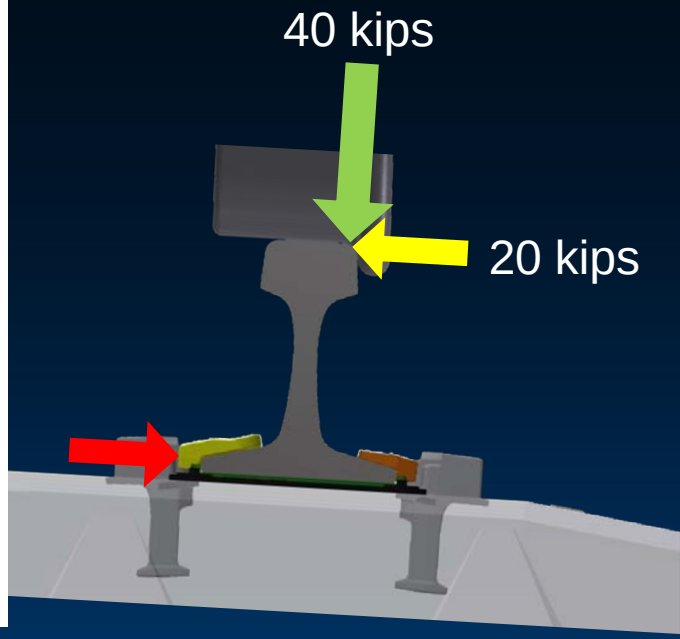

Effect of Lateral Stiffness

- A higher lateral stiffness leads to more lateral bearing load carried by that particular rail seat

Rail Seat	Lateral Stiffness (lbf/in)	Max. Force (lbf)
S	192,498	7,828
E	155,369	5,582
U	146,322	4,632

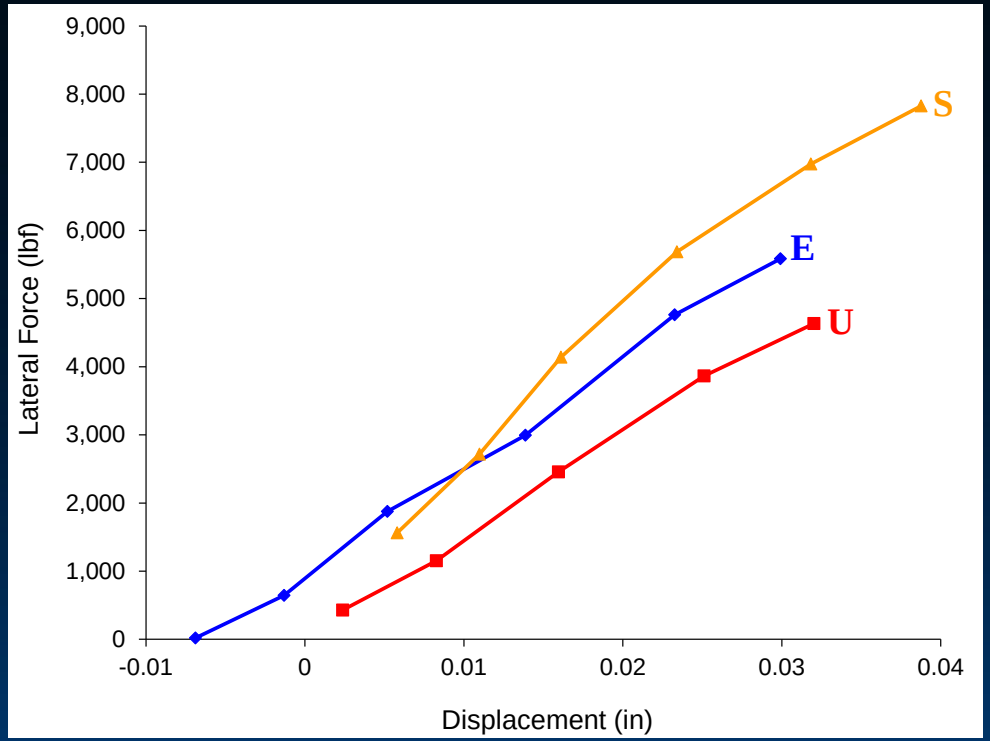

Effect of Lateral Load: Rail Seat Pressure Distribution

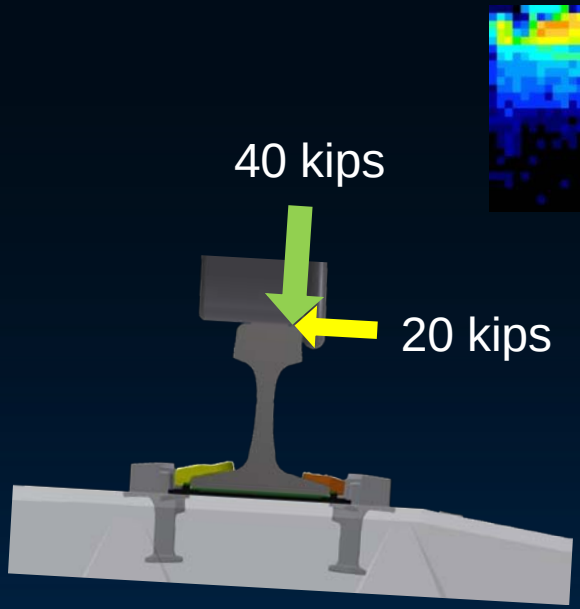

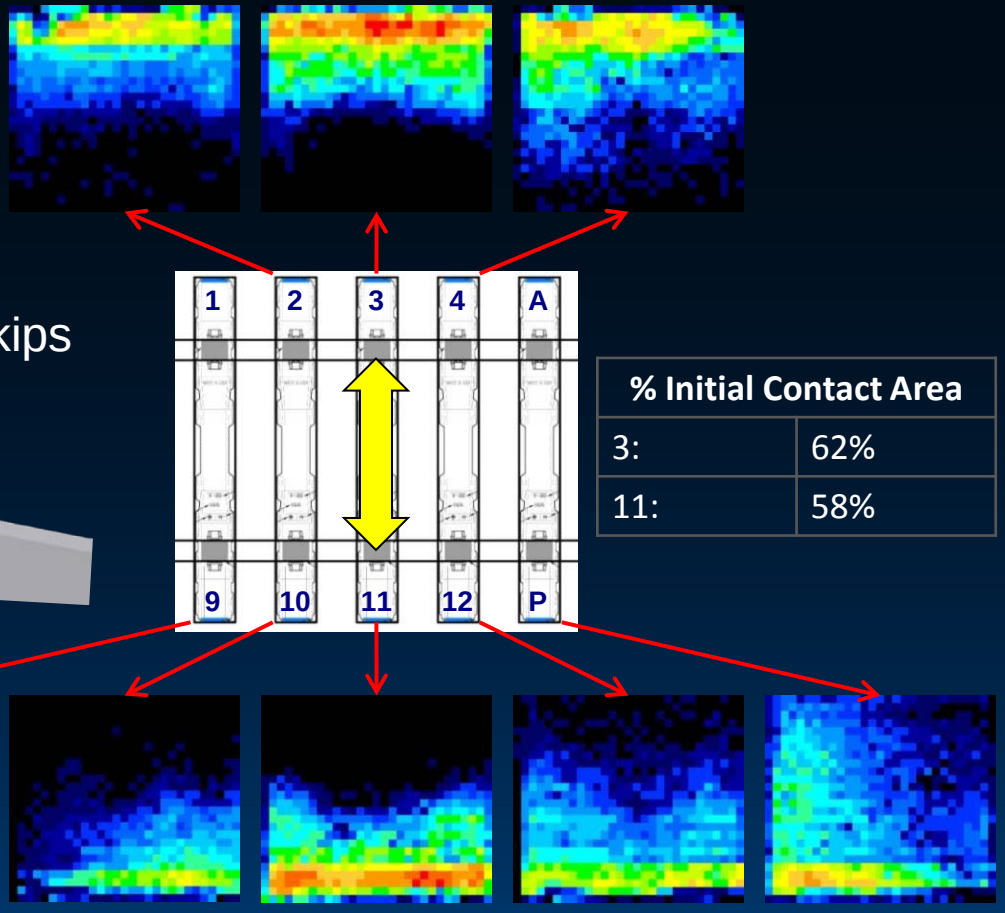

% Initial Contact Area	
3:	62%
11:	58%

Dynamic Load Input: Moving Trains

- Freight train
  - Three six-axle locomotives
  - Ten freight cars with 263k, 286k, and 315k cars
  - Speeds run at 2 mph,15 mph, 30 mph, 40 mph, and 45 mph
- Passenger train
  - One six-axle locomotive
  - Nine passenger cars
  - Speeds run at 2 mph,15 mph, 30 mph, and 40 mph
- Tested on HTL (curved section)

Dynamic Transfer of Lateral Loads:
Wheel to Fastening System

- Peak LLED and lateral wheel loads from each passing freight wheel
- Dynamic loads are applied at much higher rates than static
  - Higher bearing forces may be caused by lowered COFs due to dynamic friction

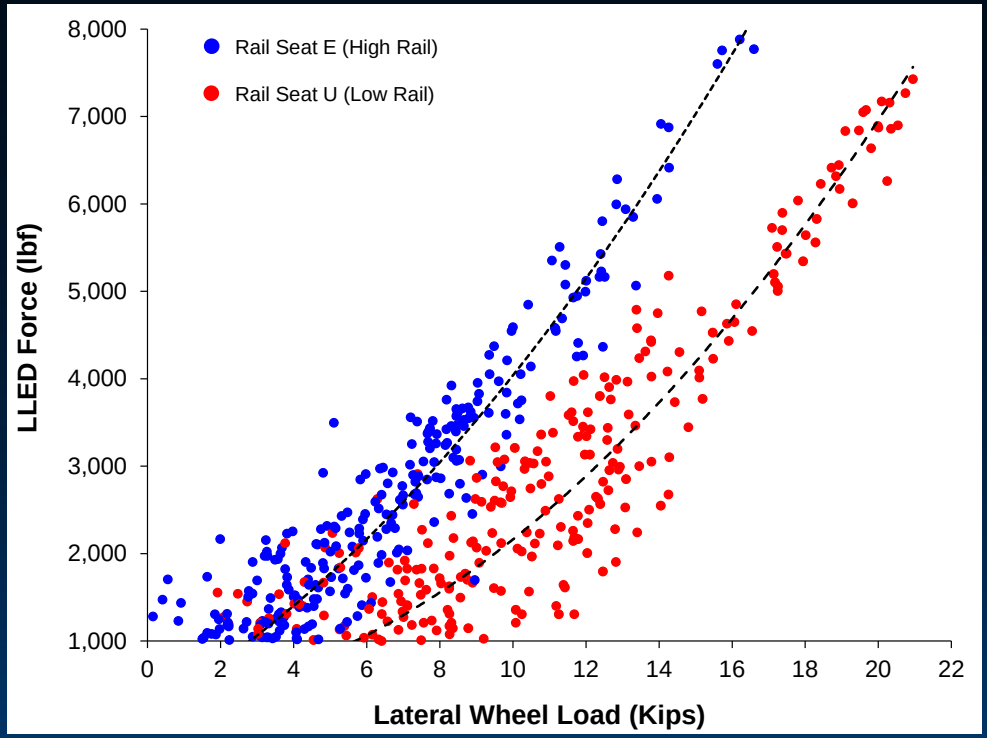

Dynamic Transfer of Lateral Loads:
Wheel to Fastening System

- Peak LLED forces as a function of speed
- As hypothesized, high rail forces increase and low rail forces decrease as speed increases
- Passenger trains yielded forces an order of magnitude lower than freight trains

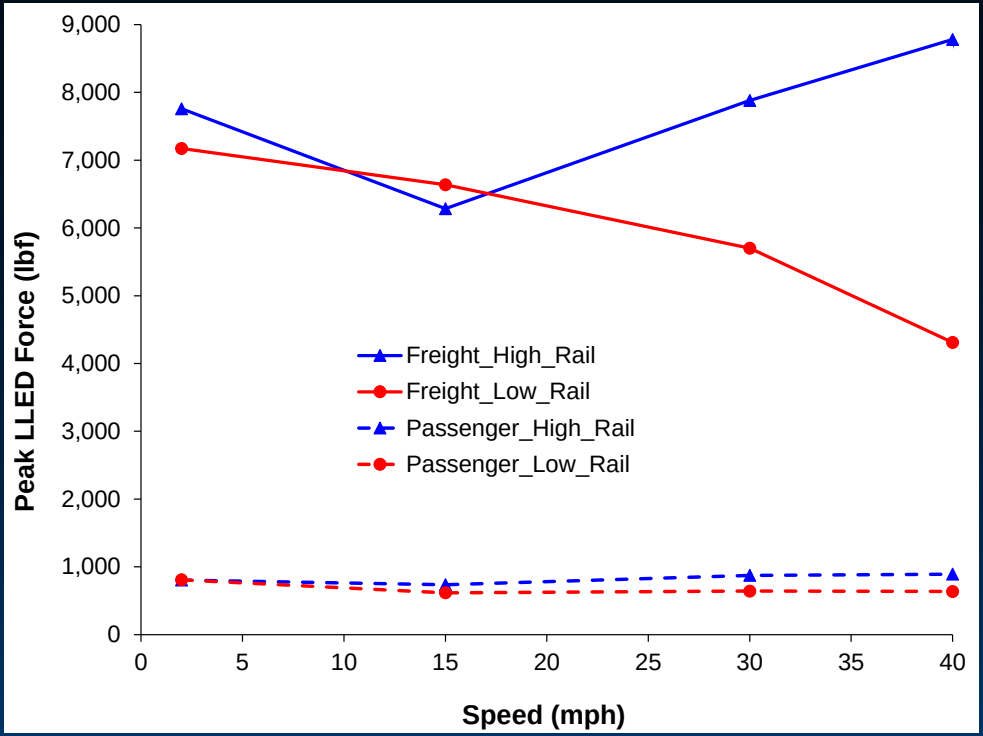

Conclusions: Static Observations

- Theoretically, decreasing vertical load should decrease frictional forces and increase bearing forces
- However, the data do not support this theoretical assumption
- Under half the vertical load, the bearing forces only increase by approximately 10%
- Future work will focus on improving upon the current lateral load model
- Rail seat pressure distribution becomes highly non-uniform as lateral load increases

Conclusions: Dynamic Observations

- A higher percentage of lateral wheel loads is transferred to the fastening system under dynamic loading than static loading
- Lateral fastening system stiffness can affect the lateral load transfer characteristics
- The percentage of lateral wheel load transferred to the shoulder increases as lateral wheel load increases
- Freight cars imparted 10x greater forces on the shoulder than passenger cars

Future Work

- Lateral load measurement on high-traffic, high-tonnage Class I track
  - What are magnitudes under true demanding field conditions?
  - What are the effects of varying track geometry?
- Full-scale laboratory testing at UIUC
  - What are the effects of varying fastening system frictional characteristics?
  - How does lateral track stability affect lateral fastening system forces?
- Component-level laboratory testing
  - What are the thresholds of plastic damage for components in the lateral load path?
  - How do alternative material properties affect load transfer and distribution of forces within the fastening system?

Acknowledgements

- **Funding for this research has been provided by:**
  - **Association of American Railroads (AAR)**
  - **Federal Railroad Administration (FRA)**
- Industry partnership and support has been provided by:
  - Union Pacific Railroad
  - BNSF Railway
  - National Railway Passenger Corporation (Amtrak)
  - Amsted RPS / Amsted Rail, Inc.
  - GIC Ingeniería y Construcción
  - Hanson Professional Services, Inc.
  - CXT Concrete Ties, Inc., LB Foster Company
  - TTX Company
- For assistance with research and lab work
  - Andrew Scheppe, UIUC Machine Shop, Harold Harrsion

Thank You

Brent Williams
Manager of Field Experimentation
bwillms3@illinois.edu

J. Riley Edwards
Senior Lecturer and Research Scientist
email: jedward2@illinois.edu

Marcus Dersch
Senior Research Engineer
email: mdersch2@illinois.edu

RAILTEC
UNIVERSITY OF ILLINOIS AT URBANA-CHAMPAIGN